Preserving the Half-Metallicity at the Heusler Alloy Co$_2$MnSi(001) Surface: A Density Functional Theory Study

S. Javad Hashemifar,[1,2] Peter Kratzer,[1,*] and Matthias Scheffler[1]

[1]*Fritz-Haber-Institut der Max-Planck-Gesellschaft, Faradayweg 4-6, D-14195 Berlin, Germany*
[2]*Department of Physics, Isfahan University of Technology, 84156 Isfahan, Iran*
(Received 19 August 2004; published 10 March 2005)

We have studied the stability, the electronic, and the magnetic properties of Co$_2$MnSi(001) thin films for 15 different terminations using density functional theory calculations. The phase diagram obtained by *ab initio* atomistic thermodynamics shows that in practice the MnSi, pure Mn, or pure Si terminated surfaces can be stabilized under suitable conditions. Analyzing the surface band structure, we find that the pure Mn termination, due to its strong surface-subsurface coupling, preserves the half-metallicity of the system, while surface states appear for the other terminations.

Heusler alloys are promising materials to be applied as spin injectors in the rapidly developing field of spin electronics (spintronics) because they belong to the materials class of magnetic half-metals. As first evidenced by first-principles calculations [1], these systems are characterized by a metallic density of electronic states at the Fermi level (ϵ_F) for one spin channel, while the states for the other spin channel display a gap at ϵ_F, leading to 100% spin-polarized metallic conductivity. Among this group, the intermetallic compound Co$_2$MnSi, a so-called full-Heusler alloy, offers special advantages: it has the highest Curie temperature amongst the known Heusler alloys ($T_c = 985$ K) [2] and a rather wide gap in the minority spin channel [3]. However, the desired half-metallic properties can be lost near surfaces or interfaces. While for spin injection the electronic structure of the half-metal-semiconductor interface is crucial [4], surfaces are more easily accessible experimentally than interfaces, and hence lend themselves to a systematic study of the factors governing the possible loss of half-metallicity. Moreover, recent interest in spin-polarized tunneling diodes and scanning tunneling microscopy [5] gives relevance to half-metallic surfaces as a research topic in its own right.

Here, we present a comprehensive theoretical investigation of the (001) surface of Co$_2$MnSi. This surface is important for envisaged epitaxial growth of Co$_2$MnSi on Ge(001) or GaAs(001), materials to which it is very closely lattice matched. So far, *ab initio* calculations have been performed only for the standard Co and MnSi terminations of Co$_2$MnSi(001) thin films [6]. In these calculations, which did not take into account any structural relaxation, it was found that the (001) surface is no longer half-metallic, and that the spin polarization at the Fermi level is negligible. Experimental work on Co$_2$MnSi thin films has so far mostly focused on preparation techniques and the crystallinity and magnetic properties of the films [7–9]. Very recently two experimental groups reported a spin polarization of about 60% at low temperatures for Co$_2$MnSi thin films [10,11].

In this Letter, we present density functional theory (DFT) calculations demonstrating that it is possible to retain the half-metallicity of Co$_2$MnSi by appropriate termination at the (001) surface. Our results have been obtained by using the WIEN2K code, a full-potential linearized augmented-plane-wave code [12]. In order to validate the appropriateness of the approximation to the exchange-correlation energy, we have calculated the bulk properties of Co$_2$MnSi both in the local-density approximation (LDA) and in the generalized gradient approximation (GGA). We found that the theoretical lattice constant of the GGA (5.63 Å) agrees well with the experimental value (5.65 Å), while LDA predicts a considerably smaller value (5.51 Å). At the experimental lattice constant, both approximations lead to a similar half-metallic density of states (DOS), with almost the same position of ϵ_F with respect to the top of the minority valence band, and a minority band gap of 0.5 and 0.7 eV within LDA and GGA, respectively. Therefore we will use GGA for the below reported thin film calculations. However, to validate important results, these have been also tested with LDA. The surfaces have been simulated using a supercell containing 15 atomic layers, a 10 Å vacuum region, and a (1×1) surface periodicity. We verified that this slab is thick enough to reproduce well the bulk values of the atom-projected DOS, as well as the bulk magnetic moments, at the center of the slab. Muffin-tin radii of 2.0 bohr for Co and Si and 2.1 bohr for Mn together with a cutoff energy for the interstitial plane-wave basis of 15.2 Ry were used. Sampling of the surface Brillouin zone was performed with a regular mesh of (12×12) **k** points, and convergence of the results was checked by comparing with a (16×16) **k**-point mesh.

The $L2_1$ structure of Co$_2$MnSi in (001) direction consists of alternating Co and MnSi planes (see Fig. 1 left), with the Mn and Si positions interchanged in subsequent MnSi planes. Therefore, there are two possible ideal MnSi and Co terminations. We have modified these two terminations by replacing the surface elements by other ele-
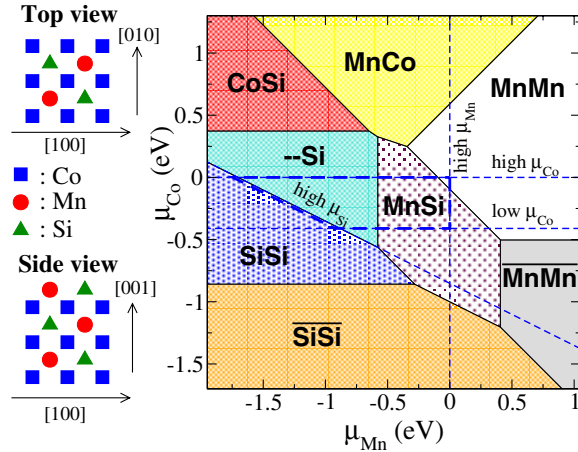
FIG. 1 (color online). Schematic top and side views of the MnSi terminated $Co_2MnSi(001)$ film (left panel), and (right panel) calculated phase diagram of $Co_2MnSi(001)$ films. The shadings indicate the regions of stability of different surface terminations; dashed lines mark the stability limits with respect to bulk materials (see text). The surfaces indicated by overlines are on a MnSi subsurface while others are on Co subsurface.

ments of the system or vacancies, leading to 15 different surface terminations of the (001) surface realized within the (1×1) unit cell, and calculated their stability within *ab initio* atomistic thermodynamics. The four terminations found to be stable are discussed in more detail: MnSi, MnMn (replacing Si with Mn in the MnSi surface), SiSi (replacing Mn with Si in the MnSi surface), −Si (replacing Mn with a vacancy in the MnSi surface), where in all cases the subsurface layer consists of Co atoms. In the calculations, the atomic positions are fully relaxed, except the atoms in the five central layers of the slab.

In *ab initio atomistic thermodynamics* [13,14], the surface free energy, $\gamma(T, p_i) = [G(T, p_i) - \Sigma_i N_i \mu_i(T, p_i)]/A$ obtained from DFT calculations is used to assess the stability of a particular surface termination. Here, G is the Gibbs free energy of the film, N_i and μ_i are the number and the chemical potential of the ith element, and γ is the free energy per unit of surface area. Since we like to consider surfaces that are in thermodynamic equilibrium with the bulk, two *independent* chemical potentials are sufficient to describe the dependence of surface stability under varying experimental conditions. We select the chemical potential of Co and Mn, because, in experiments, the evaporation of Co and Mn is simpler than that of Si, and therefore changes of μ_{Co} and μ_{Mn} in the grown film can be achieved by depositing under slightly nonstoichiometric conditions. The phase diagram shows the surface with the lowest surface free energy for a given pair of values (μ_{Co}, μ_{Mn}). As discussed in other studies [14], it is often a good approximation to calculate surface free energies from the *differences* of DFT total energies alone, namely, when vibrational contributions to the free energy can be assumed to cancel out. We have tested this assumption for our system using the Debye model for the phonon spec-

trum. The Debye temperature of Mn, Co, and bulk Co_2MnSi is 410, 445, and 456 K, respectively [15,16], and for the slab we use the general rule that the Debye temperature at the surfaces decreases about 50%–70% with respect to the bulk value [17]. Our results show that below 400 K the vibrational contribution to the surface free energy is less than 20 meV/Å², while around 1000 K it reaches about 50 meV/Å². By comparing to typical surface energies (~150 meV/Å²), we conclude that the general features of the phase diagram are valid up to temperatures of about 400 K. The accessible region of the phase diagram is limited by the Gibbs free energies of other bulk materials that can be formed. For example, if μ_{Co} becomes low the sample would decompose into bulk MnSi and elementary Co droplets. The low μ_{Co} limit corresponds to $\mu_{Mn} + \mu_{Si} = g_{MnSi}$, from which $\mu_{Co} \geq (g_{Co_2MnSi} - g_{MnSi})/2$ is derived by eliminating μ_{Si} using the Gibbs free energy of the bulk Heusler alloy. Similarly, the following boundaries of the admissible region in the phase diagram can be derived from other limits for the chemical potentials: formation of bulk Mn (high μ_{Mn}), bulk Co (high μ_{Co}), bulk Si (low $\mu_{Co} + \mu_{Mn}$), and bulk CoSi and $CoSi_2$ (low μ_{Mn}). To calculate these limits, we have computed the theoretical ground state energy of all these materials accurately, except for the CoSi compounds where literature data show them to lie well outside the accessible region of the phase diagram. For the complicated magnetic ground state of bulk Mn (α-Mn), we apply a correction taken from Ref. [18] to our calculated energy of antiferromagnetic γ-Mn to obtain the true ground state energy of α-Mn. We note that the regions outside the stability limits could still be reached in experiment by sufficiently fast nonequilibrium growth.

Figure 1 shows the calculated phase diagram of the various considered surfaces. In addition to the cases listed in the figure, we have considered five other surfaces (CoCo, CoSi, CoMn, and Co− surfaces on a MnSi subsurface layer, and Mn− on a Co subsurface layer) and found all of them to be unstable with respect to other terminations that appeared in the phase diagram. Moreover, for the MnMn surfaces we have considered both ferromagnetic and antiferromagnetic ordering of the Mn magnetic moments, and found that on a Co subsurface layer, inter- and intra-planar ferromagnetic coupling is preferred, while on a MnSi subsurface layer antiferromagnetic coupling with the subsurface Mn atoms is favorable. The phase diagram clearly shows that most parts of the accessible region (bound by thick dashed lines in Fig. 1) are realized by the MnSi and −Si terminations. However, for Si-poor conditions the MnMn termination can be stabilized. This observation has important implications for the magnetic and electronic properties of the surface, as we will see below. Furthermore, the SiSi termination may be stable for very Si-rich conditions.

In Table I, we list various calculated parameters for the four stable terminations. The clear enhancement in the magnetic moment of the Mn atoms at the surfaces with

respect to the bulk value is due to the well-known effect of symmetry breaking at the surface. The reduced number of Co neighbors at the surface leads to a rehybridization of the Mn atom, and thus to a transfer of almost half of its spin-down d electrons into the spin-up channel, resulting in an increased magnetic moment. The magnetization of the subsurface Co atoms, in all cases except the −Si surface, is close to the bulk value, and increases slightly by increasing the number of Mn atoms at the surface. In the bulk Co$_2$MnSi, Si has a weak magnetic moment antiparallel to the Mn atoms, and at the MnSi surface, enhancement of the magnetic moment of Mn increases slightly the magnetic moment of Si in the opposite direction. We calculate the surface spin polarization at the Fermi level P_S from the DOS projected onto the atomic orbitals of both the surface and subsurface atoms. As a general trend, we see that it increases by increasing the number of Mn atoms at the surface. The negligible value of the surface buckling Δz for the MnMn surface indicates the high smoothness of this
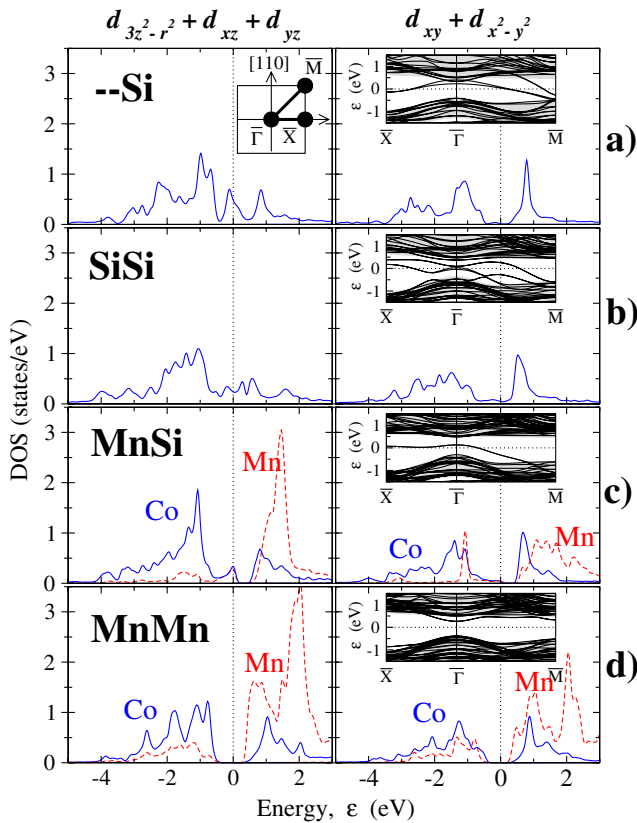

FIG. 2 (color online). The electronic structure of (a) −Si, (b) SiSi, (c) MnSi, and (d) MnMn surfaces. Left and right panels: spin-down d partial DOS of the surface Mn (red, dashed) and subsurface Co atoms (blue) for the d orbitals out of plane ($3z^2 - r^2$, xz, yz) and in plane (xy, $x^2 - y^2$). The energy zero is the Fermi level, ϵ_F. Inset left panel (a): two-dimensional reciprocal lattice of the films. Insets right panel: minority spin band structure; the shaded area represents the minority spin bulk bands projected onto the (001) plane.

surface. The outstanding result in this Table is the half-metallic character of the Mn-capped film.

Next, we turn to the electronic structure of the different surface terminations. As the main result, Fig. 2 displays the DOS of minority spin of Co$_2$MnSi films, for all terminations found to be stable. In all cases surface states located in the minority spin gap are detected.

For the stable standard surface, the MnSi termination, a single surface band appears which crosses the Fermi level [see Fig. 2(c)], and hence destroys half-metallicity. In the partial DOS, it shows up as a peak right at the Fermi level, mostly derived from Co d states, while a small energy gap persists above the Fermi level. We note that the sharpness of this peak renders the surface spin polarization in this system very sensitive to the accurate position of the Fermi level. We attribute discrepancies between published calculations [6,19] of the spin polarization to this sensitivity.

For the pure Si surfaces (−Si and SiSi), we find that the minority spin gap is completely filled by three surface state bands, two of them crossing the Fermi level [see Fig. 2(a) and 2(b)]. In the case of the −Si surface, similar to the MnSi surface, we observe a sharp peak almost at the Fermi level that leads to a negative surface spin polarization (Table I), while due to the larger dispersion of the surface states at the Fermi level the spin polarization at the SiSi surface almost vanishes. At the MnMn surface, however, a well-defined gap persists at the surface, and the Fermi level is located inside this gap, which makes the film an ideal half-metal. Surface states show up only in limited regions of the surface Brillouin zone: an unoccupied state, predominantly derived from Mn d orbitals, arises around the $\overline{\Gamma}$ point (in LDA we found that this state starts to be occupied). The partially filled, Co-derived surface state present for MnSi termination has turned into a surface resonance for this system and can only be observed near the $\overline{X}$ point [see Fig. 2(d)].

In order to understand how a specific surface termination affects the half-metallicity, we need to discuss the electronic structure of the Co$_2$MnSi full-Heusler alloy in qualitative terms. While the Si sp orbitals contribute to the bonding states far below the Fermi level, the electronic states around ϵ_F are almost entirely derived from the metal

TABLE I. Calculated surface properties of the Co$_2$MnSi thin films: magnetic moments m of the surface atoms (X and Y) and subsurface Co atoms for different XY terminations; surface spin polarization P_S and vertical distance Δz between atoms X and Y after relaxation. For the bulk, X and Y correspond to Mn and Si atoms, respectively.

Termination (XY)	−Si	SiSi	MnSi	MnMn	Bulk
$m_X(\mu_B)$	⋯	+0.05	+3.59	+3.63	+2.91
$m_Y(\mu_B)$	−0.06	−0.02	−0.09	+3.65	−0.04
$m_{Co}(\mu_B)$	+0.52	+0.91	+0.98	+1.17	+1.07
P_S	−17%	−3%	−16%	100%	⋯
Δz (Å)	−0.33	−0.24	+0.29	−0.01	⋯

d orbitals. We restrict the discussion to minority spin orbitals, and first observe that the minority d states of Mn are generally shifted to higher energies compared to the d orbitals of Co due to stronger exchange splitting at the Mn atoms. Hence the two types of d orbitals only partially mix with each other. As evidenced by the integer total magnetic moment of $5\mu_B$ per unit cell of Co_2MnSi, the number of unoccupied bands in the minority spin channel exceeds those in the majority spin channel by five. Most of the amplitude of these unoccupied states comes from Mn d orbitals. In contrast, the states directly above and below the minority spin gap are found to have mostly Co d character. Our findings are in agreement with earlier observations by Galanakis *et al.* [20], which ascribe the half-metallic band gap of the bulk material to the energy splitting between Co-derived t_{1u} and e_u orbitals. At the surface, the symmetry is reduced, leading to a rehybridization among the d orbitals. We analyze the electronic structure in terms of groups of d orbitals in the surface plane and out of plane.

As clearly seen from Fig. 2, the surface states in the band gap originate from out-of-plane d orbitals. The analysis is most easy for the pure Si surfaces: the surface Si atoms, with their sp states at rather low energies, cannot act as efficient hybridization partners for the subsurface Co atoms that have lost their Mn neighbors. Thus the surface states arise mainly from dangling $d_{3z^2-r^2}$ orbitals of the (subsurface) Co layer, with some admixture of Si sp_z hybrid orbitals. For the MnSi surface, the surface Mn atoms have lost half of their Co neighbors (compared to bulk). This results in rehybridization which raises the $d_{3z^2-r^2}$ orbital of Co up to the Fermi level, transforming it to a partially filled surface state. This interpretation is supported by analyzing the electronic structure of the *half* Heusler alloy CoMnSi (using the lattice constants of Co_2MnSi) where in analogy with the MnSi surface, Mn has only one Co partner. In this case, a similar state, formed from Co $d_{3z^2-r^2}$ orbitals and Mn d_{xz} and d_{yz} orbitals, occurs as an occupied bulk state. In the present case of a thin film, however, the electrostatic potential falling off towards the vacuum region lifts this state to the Fermi level, thus breaking the half-metallic character. The differences between bulk and surface electronic structure are most pronounced for the MnMn surface. Here, the Co subsurface atoms each interact with *two* Mn atoms in the surface layer. While the overall number of spin-down electrons per atom located in d orbitals of both the Mn and Co layers is nearly the same as for the MnSi surface, these electrons are now accommodated in bands of Mn d_{xy} and Co d_{xz} and d_{yz} character [see Fig. 2(d)], which are well below the Fermi level. Hence, the half-metallic character of the bulk material is retained at the surface.

In summary, our calculations show that the half-metallic properties of the bulk Co_2MnSi Heusler alloy need not be destroyed at surfaces. Spin-polarized STM studies would be very useful to test this prediction. Moreover, our detailed investigations of the surface electronic structure call for photoemission experiments on well-prepared films. In particular, the closely lattice matched system $Co_2MnSi(001)/GaAs(001)$, together with a Mn interface layer, may be a promising candidate structure for spin injection, notwithstanding recent computational studies [21] where this possibility was not considered.

*Electronic address: kratzer@fhi-berlin.mpg.de

[1] R. A. de Groot, F. M. Mueller, P. G. van Engen, and K. H. J. Buschow, Phys. Rev. Lett. **50**, 2024 (1983).

[2] P. J. Brown, K. U. Neumann, P. J. Webster, and K. R. A. Ziebeck, J. Phys. Condens. Matter **12**, 1827 (2000).

[3] S. Ishida, S. Fujii, S. Kashiwagi, and S. Asano, J. Phys. Soc. Jpn. **64**, 2152 (1995).

[4] G. A. de Wijs and R. A. de Groot, Phys. Rev. B **64**, 020402 (2001).

[5] O. Pietzsch, A. Kubetzka, M. Bode, and R. Wiesendanger, Appl. Phys. A **78**, 781 (2004).

[6] I. Galanakis, J. Phys. Condens. Matter **14**, 6329 (2002).

[7] M. P. Raphael *et al.*, Appl. Phys. Lett. **79**, 4396 (2001).

[8] S. Kämmerer *et al.*, J. Appl. Phys. **93**, 7945 (2003).

[9] U. Geiersbach, A. Bergmann, and K. Westerholt, J. Magn. Magn. Mater. **240**, 546 (2002).

[10] S. Kämmerer, A. Thomas, A. Hütten, and G. Reiss, Appl. Phys. Lett. **85**, 79 (2004).

[11] L. J. Singh, Z. H. Barber, Y. Miyoshi, W. R. Branford, and L. F. Cohen, J. Appl. Phys. **95**, 7231 (2004).

[12] K. Schwarz and P. Blaha, Comput. Mater. Sci. **28**, 259 (2003).

[13] K. Reuter, C. Stampfl, and M. Scheffler, in "Handbook of Materials Modeling," edited by S. Yip (Kluwer, Dordrecht, to be published), and references therein. URL: http://www.fhi-berlin.mpg.de/th/pub05.html.

[14] K. Reuter and M. Scheffler, Phys. Rev. B **65**, 035406 (2001).

[15] C. Kittel, *Introduction to Solid State Physics* (Wiley, New York, 1996), 7th ed.

[16] For Co_2MnSi we have used its theoretical bulk modulus, $B = 221$ GPa, to calculate the speed of sound, $v_s = \sqrt{B/\rho}$, ρ: density, and the Debye temperature $\theta_D = (\hbar v_s/k_B)(6\pi^2 N/V)^{1/3}$, N: number of atoms in crystal, V: crystal volume, k_B: Boltzmann constant.

[17] A. Zangwill, *Physics at Surfaces* (Cambridge University Press, Cambridge, England, 1988).

[18] J. Hafner and D. Hobbs, Phys. Rev. B **68**, 014408 (2003).

[19] S. Ishida, T. Masaki, S. Fujii, and S. Asano, Physica B (Amsterdam) **245**, 1 (1998).

[20] I. Galanakis, P. H. Dederichs, and N. Papanikolaou, Phys. Rev. B **66**, 174429 (2002).

[21] S. Picozzi, A. Continenza, and A. J. Freeman, J. Phys. Chem. Solids **64**, 1697 (2003).